EFFECT OF FCC-ee OPTICS ERRORS IN COLLISION SIMULATED BY XSUITE*

V. Gawas†[1,2], X. Buffat[1], P. Kicsiny‡[1,3], F. Zimmermann[1]
[1]CERN, Geneva, Switzerland
[2]University of Geneva, Geneva, Switzerland
[3]École Polytechnique Fédérale de Lausanne, Lausanne, Switzerland

Abstract

The luminosity performance of FCC-ee is sensitive to spurious optics errors at the Interaction Point (IP), notably to nonzero waist shift, vertical dispersion, and transverse coupling. Using the code Xsuite, we study how these aberrations influence beam sizes, luminosity, and beamstrahlung power, for the FCC-ee baseline parameters. Multi-turn simulations have been carried out to study the equilibrium distribution/dynamics. Simulated sensitivities for linear lattice descriptions allow an assessment regarding the impact of strong-strong beam-beam effects on IP tuning. By scanning the amplitude of individual linear IP optics aberrations, we infer tolerance estimates for which the simulated performance remains compatible with the design expectations. We compare these with the results of earlier (single-pass) simulations by the code GUINEA-PIG and with analytical calculations. Our study aims at providing a consistent picture of beam–beam behaviour at the FCC-ee IP, so as to help devise future strategies for luminosity optimisation and IP tuning.

INTRODUCTION

We are investigating how spurious optics errors at the FCC-ee interaction point affect beam–beam dynamics, luminosity, and beamstrahlung at the $t\bar{t}$ working point (182.5 GeV centre of mass energy) [1, 2]. Our study is based on self-consistent multiturn beam-beam simulations performed with the code `Xsuite` [3]. These simulations should provide guidance for the beam–beam-based tuning and Bayesian optimization strategies to be developed for FCC-ee [4]. The FCC-ee is designed to operate close to the beam–beam limit in order to achieve extremely high luminosity [1]. Under these conditions, small optics errors at the interaction point can lead to significant degradation of performance. In particular, three classes of low-order IP aberrations are known to be critical: longitudinal shifts of the vertical waist, residual vertical dispersion, and transverse coupling. Such aberrations were previously observed and corrected with some success, e.g., at the SLAC Linear Collider (SLC) [5], at KEKB [6], and at SuperKEKB [7]. The IP optics errors fluctuate and drift due to changes in the ring circumference, temperature variation, orbit changes, ground motion, and beam-dynamics effects, and must, therefore, be controlled by beam-beam-based feedback and tuning.

* This work was supported by the Swiss CHART programme.
† vaibhavi.gawas@cern.ch
‡ Now at SLAC National Accelerator Laboratory, Menlo Park, CA, USA.

Simulation Framework

In the `Xsuite` tracking code, we represent the FCC-ee lattice by a linear transport model between a final focus element, e.g., a crab-waist sextupole, and a single interaction point (IP), and by the inverse linear transport on the other side of the IP. Beam-beam interactions are modeled through nonlinear sliced kicks applied once per turn. Radiation damping and quantum excitation are included [8]. Controlled waist shifts, dispersion, and coupling are then introduced by modifying the linear transport matrices at the IP. Multi-turn simulations have been carried out to study the equilibrium distribution/dynamics, as is illustrated in Fig. 1 for various cases of spurious vertical dispersion at the IP. The simulation models the combined effects of radiation damping, beam-beam forces, beamstrahlung-induced energy spread, and IP aberration.

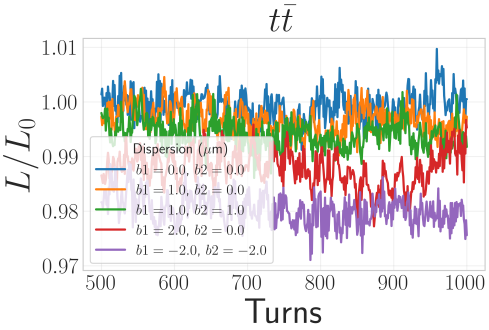

Figure 1: Luminosity evolution up to 1000 turns, with spurious vertical IP dispersion for the two beams, as indicated.

Each IP aberration is varied independently around the design working point, while all other parameters are kept fixed. The resulting luminosity and beamstrahlung power levels (calculated from beamstrahlung energy at every turn) are then recorded as functions of the aberration amplitude. This procedure allows tolerance ranges to be defined for which the performance remains compatible with the FCC-ee design goals.

Waist shift. In the absence of errors, the vertical beta function has a minimum at the IP. A longitudinal shift z_0 of the waist leads to an increase of the IP beta function according to $\beta^*_y(z) = \beta^*_{y,0} + (z - z_0)^2/\beta^*_{y,0}$, which increases the effective beam size in the collision region. Since the bunch has a finite length, a nonzero z_0 reduces the overlap of the two beams and degrades luminosity, particularly in the presence of strong beam-beam focusing and hourglass effect.

Vertical dispersion. A residual vertical dispersion D_y^* causes particles with different energies to collide at different vertical positions. The resulting increase in the mean-square vertical beam size is given by

$$\sigma_y^{*,2} = \beta_y^* \varepsilon_y + (D_y^* \sigma_\delta)^2,$$

where σ_δ denotes the rms relative energy spread. Even for small values of D_y^*, the term $D_y^* \sigma_\delta$ can dominate over the intrinsic vertical betatron beam size $(\beta_{y,0}^* \varepsilon_y)^{1/2}$ and strongly reduce luminosity.

Transverse coupling. Linear betatron coupling mixes horizontal and vertical motion, allowing part of the large horizontal emittance to leak into the vertical plane. This is described by a coupled transport matrix from crab-sextupole to the IP [9, 10],

$$\begin{pmatrix} X \\ Y \end{pmatrix}_2 = \begin{bmatrix} \gamma_2 I & C_2 \\ -C_2^+ & \gamma_2 I \end{bmatrix} \begin{pmatrix} A_{12} & 0 \\ 0 & B_{12} \end{pmatrix} \begin{bmatrix} \gamma_1 I & -C_1 \\ C_1^+ & \gamma_1 I \end{bmatrix} \begin{pmatrix} X \\ Y \end{pmatrix}_1 .$$

where the coupling matrix C and γ are functions of $(\alpha_x, \beta_x, \alpha_y, \beta_y, f_{1001}, f_{1010})$, with f_{1001} and f_{1010} referring to resonance driving terms [10].

LUMINOSITY TOLERANCES

Approximate Analytical Estimates

The luminosity is inversely proportional to the vertical rms beam size at the IP: $\mathcal{L} \propto 1/\sigma_y^*$. Therefore, an increase in vertical beam size from $\sigma_{y,0}$ to $\sigma_y^* = \sigma_{y,0}^*(1 + \Delta\sigma_y/\sigma_{y,0}^*)$ reduces the luminosity to

$$\frac{\mathcal{L}}{\mathcal{L}_0} = \frac{1}{1 + \Delta\sigma_y/\sigma_{y,0}^*} \approx 1 - \Delta\sigma_y/\sigma_{y,0}^*,$$

with $\Delta\sigma_y/\sigma_{y,0}^* \ll 1$. Requiring a tolerable luminosity loss Δ yields the condition $\Delta\sigma_y/\sigma_{y,0}^* < \Delta$.

Vertical waist shift. At the $t\bar{t}$ working point, $\kappa_y \equiv \sigma_z/\beta_y^* = 1.33$, i.e. the hourglass effect becomes relevant [11, 12]. This introduces an effective overlap region of rms extent given by $\sigma_{z,\mathrm{eff}} = \sigma_z/\sqrt{2(1+\Phi^2)}$, with $\Phi \equiv \sigma_z \theta_c/(2\sigma_x^*)$ the Piwinski angle, and θ_c the full crossing angle. The luminosity loss due to a vertical waist shift Δs_y, in the same physical direction for both beams ("overlap"), is given by the following ratio of hourglass integrals [11]:

$$\frac{\mathcal{L}(\Delta s_y)}{\mathcal{L}_0} = \frac{\displaystyle\int_{-\infty}^{\infty} \frac{e^{-z^2/\sigma_{z,\mathrm{eff}}^2}}{1 + (z - \Delta s_y)^2/\beta_y^{*2}}\, dz}{\displaystyle\int_{-\infty}^{\infty} \frac{e^{-z^2/\sigma_{z,\mathrm{eff}}^2}}{1 + z^2/\beta_y^{*2}}\, dz}.$$

This yields tolerances of $|\Delta s_y| \lesssim 0.35\,\mathrm{mm}$ for 1% and $|\Delta s_y| \lesssim 0.79\,\mathrm{mm}$ for 5% luminosity loss, respectively.

Horizontal waist shifts are found to have negligible impact on luminosity in simulations, due to the large β_x^*.

Vertical dispersion. Vertical dispersion (D_y^*) and its derivative ($D_y^{*\prime}$) at the IP increase the beam size as $\sigma_y = \sqrt{\varepsilon_y \beta_y^* + (D_y^* \sigma_\delta)^2}$ and $\sigma_y = \sqrt{\varepsilon_y \beta_y^* + (D_y^{*\prime} \sigma_{z,\mathrm{eff}} \sigma_\delta)^2}$, respectively. Applying the condition $\Delta\sigma_y/\sigma_{y,0}^* < \Delta$ gives $|D_y^*| < \sigma_{y,0}\sqrt{2\Delta}/\sigma_\delta$ and $|D_y^{*\prime}| < \sigma_{y,0}\sqrt{2\Delta}/(\sigma_\delta \sigma_{z,\mathrm{eff}})$, yielding $|D_y^*| \lesssim 3.2\,\mu\mathrm{m}$ and $7.3\,\mu\mathrm{m}$, and $|D_y^{*\prime}| \lesssim 2.3\,\mathrm{mrad}$ and $5.2\,\mathrm{mrad}$ for 1% and 5% luminosity loss, respectively. Horizontal dispersion tolerances are quite relaxed due to the large horizontal beam size and are not limiting performance.

Transverse coupling. Coupling increases the effective vertical emittance as $\varepsilon_{y,\mathrm{eff}} = \varepsilon_y + 8\left(|f_{1001}|^2,\ |f_{1010}|^2\right)\varepsilon_x$ [9, 13]. The luminosity constraint gives, e.g.,

$$|f_{1001}|,\ |f_{1010}| < \frac{1}{2}\sqrt{\frac{\varepsilon_y}{\varepsilon_x}}\sqrt{\Delta}.$$

This yields $|f_{1001}| \lesssim 1.5 \times 10^{-3}$ (1%) and $|f_{1001}| \lesssim 3 \times 10^{-3}$ (5%). The same analytical tolerance applies to $|f_{1010}|$, although in simulations the inherent instability of the sum resonance [14] leads to a stronger degradation.

Simulated Tolerances

We simulate individual IP aberrations and quantify their impact on luminosity through 2D parameter scans over the aberration amplitudes for beam 1 (B1) and beam 2 (B2). Figure 2 shows the normalized luminosity as a function of vertical dispersion, waist shift, difference resonance coupling f_{1001}, and sum resonance coupling f_{1010}.

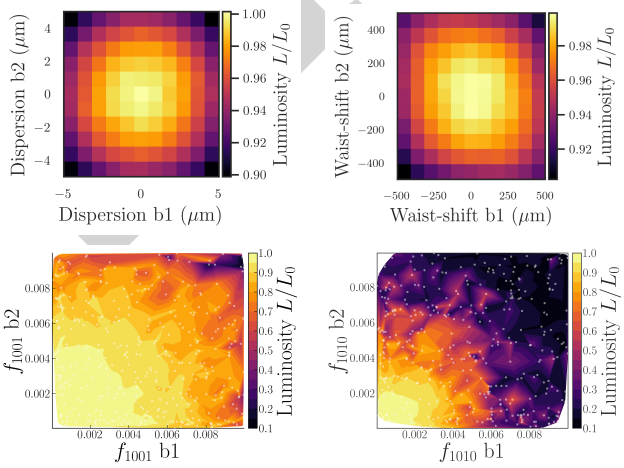

Figure 2: Normalized luminosity dependence on IP aberrations at $t\bar{t}$ running, corresponding to a beam energy of 182.5 GeV, with full beam–beam interaction. The luminosity is averaged over turns 800–1000 and normalized to the aberration-free value.

For the vertical beam waist, the maximum luminosity is achieved when the waists of the beams overlap at the IP, as expected. When the waist of Beam 1 is shifted downstream (upstream) and that of Beam 2 is shifted upstream (downstream) by the same amount in their respective reference frames, the waists no longer overlap at the IP but instead intersect at a displaced longitudinal position. This allows a relatively better overlap of the beam densities and results in higher luminosity compared to when both beams are

shifted upstream (or downstream). Nevertheless, luminosity losses arise even from purely longitudinal waist offsets: at $|\Delta w_y| \sim \pm 100\,\mu$m losses reach ~1%, increasing to 2–3% at $\sim \pm 300\,\mu$m.

Table 1: Analytical And Simulated Luminosity-Loss Tolerances

	Analytical		Simulation	
Aberration	**1%**	**5%**	**1%**	**5%**
$\lvert\Delta s_y\rvert$	0.35 mm	0.79 mm	0.2 mm	0.4 mm
$\lvert D_y^*\rvert$	3.9 μm	8.8 μm	1.0 μm	3.0 μm
$\lvert D_y^{*\prime}\rvert$	2.8 mrad	6.3 mrad	1.0 mrad	2.0 mrad
$\lvert f_{1001}\rvert$	1.5×10^{-3}	3.0×10^{-3}	2.0×10^{-3}	4.0×10^{-3}
$\lvert f_{1010}\rvert$	1.5×10^{-3}	3.0×10^{-3}	1.0×10^{-3}	2.0×10^{-3}
$\lvert D_x\rvert$	2.9 mm	6.4 mm	2.0 mm	5.0 mm
$\lvert D_x'\rvert$	3.2 mrad	7.1 mrad	2.0 mrad	4.0 mrad

Vertical dispersion imposes more stringent constraints. Even a perturbation of 1 μm causes a ~1% luminosity drop, growing to ~10% at 5 μm, reflecting the sensitivity of the tiny vertical emittance to energy-dependent orbit offsets. Concerning linear coupling effects, the sum resonance (f_{1010}) at an amplitude of $\sim 2\times10^{-3}$ causes ~2% luminosity loss, while the difference resonance (f_{1001}) at the same amplitude causes ~1% degradation, as detailed in [10]. This is especially concerning since current estimates of the expected machine coupling are of the same order of magnitude, highlighting the need for precise IP tuning [15]. For completeness, we also look at the impact of horizontal dispersion. The tolerances are less tight given the micro-meter scale in the horizontal plane. The thresholds derived from these scans, defined as the aberration amplitude at which luminosity loss does not exceed ~1% or ~5% for each effect individually, are summarised in Table 1.

Beam-size and Beamstrahlung

All aberrations primarily degrade luminosity through an increase of the effective vertical beam size. For vertical waist shifts, the beam size increases due to collisions occurring away from the waist over the finite bunch length. An asymmetry is observed, forward shifts produce a stronger increase than backward shifts, reflecting the interplay with beam–beam focusing.

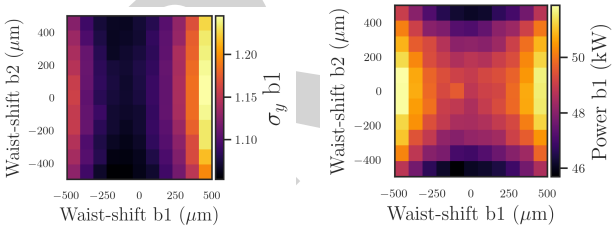

Figure 3: Dependence of the normalized vertical beam size (left) and beamstrahlung power (right) on the waist shift.

The beamstrahlung power as shown in Fig. 3 follows a correlated but asymmetric behaviour. Increasing the waist shift

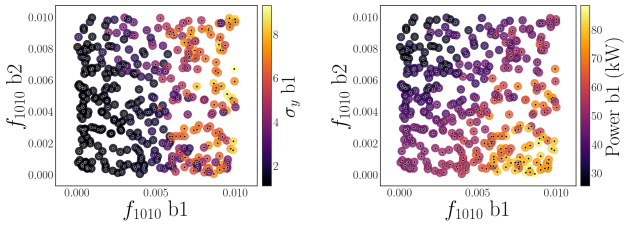

Figure 4: Dependence of the normalized vertical beam size (left) and beamstrahlung power (right) on f_{1010}.

in one beam enhances its emitted power, while a shift in the opposing beam reduces it. This indicates that beamstrahlung is sensitive not only to beam size, but also to the longitudinal overlap and local beam–beam strength.In case of sum resonance coupling as shown in Fig.4, we see similar effects. As the vertical size of beam-1 grows its beamstrahlung emission increases. While increasing the coupling in beam-2 weakens the beam-beam force experienced by beam-1 and leads to lower beamstrahlung emissions.

Comparison with Guinea-Pig

The single-pass simulations (Fig. 5) from GUINEA-PIG reproduce the same qualitative trends as `Xsuite`, including the asymmetry of luminosity with respect to waist shift and the position of the maximum at waist overlap. However, GUINEA-PIG predicts systematically smaller luminosity degradation. This is due to the absence of multi-turn effects such as radiation damping, energy spread evolution, and cumulative beam–beam interactions. In `Xsuite`, these effects lead to a self-consistent equilibrium distribution, where beam-size growth and beamstrahlung reinforce each other, resulting in stronger sensitivity to IP aberrations. Thus, while single-pass simulations capture the main trends, multi-turn simulations are essential for realistic tolerance estimates.

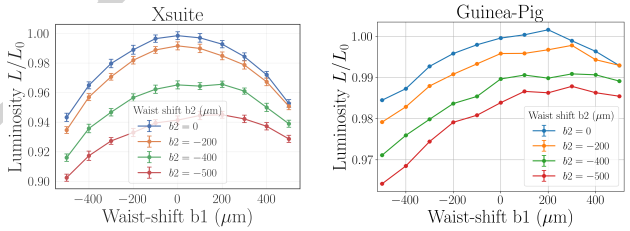

Figure 5: Normalized luminosity dependence on the waist shift in Xsuite and GUINEA-PIG. The luminosity is averaged over turns 800–1000 in Xsuite and over five repeats in GUINEA-PIG.

CONCLUSION

Executing multi-turn beam-beam simulations in `Xsuite`, we have studied the sensitivity of FCC-ee luminosity at the $t\bar{t}$ working point to three classes of linear IP aberrations: waist shift, vertical dispersion, and transverse coupling. The simulations reveal tight tolerances on all three aberration types, with vertical dispersion being the most stringent. The combined effect of realistic residual aberrations affecting the

vertical beam size is estimated to reduce the luminosity by at least 5%, motivating the development of robust beam-beam-based IP tuning and Bayesian optimisation strategies [4].

REFERENCES

[1] M. Benedikt *et al.*, "FCC-ee: the Lepton Collider: Future Circular Collider Conceptual Design Report, Volume 2", *Eur. Phys. J. Spec. Top.*, vol. 228, pp. 261–623, 2018.

[2] M. Benedikt, F. Zimmermann, B. Auchmann, *et al.*, "Future Circular Collider Feasibility Study Report, Volume 2 Accelerators, Technical Infrastructure and Safety", *Eur. Phys. J. Spec. Top.*, vol. 234, pp. 5713–6197, 2025. doi:10.1140/epjs/s11734-025-01967-4

[3] G. Iadarola *et al.*, "Xsuite: An Integrated Beam Physics Simulation Framework", in *Proc. HB'23*, Geneva, Switzerland, pp. 73–80, Mar. 2024. doi:10.18429/JACoW-HB2023-TUA2I1

[4] V. Gawas, V. Kain, and F. Zimmermann, "Bayesian optimization for IP aberration correction and luminosity tuning in FCC-ee", in *Proc. IPAC'25*, Taipei, Taiwan, pp. 290–293, Nov. 2025. doi:10.18429/JACoW-IPAC2025-MOPM011

[5] P. Emma, L. J. Hendrickson, P. Raimondi, and F. Zimmermann, "Limitations of Interaction-Point Spot-Size Tuning at the SLC", in *Proc. PAC'97*, Vancouver, Canada, May 1997, paper 5B007, pp. 452–454.

[6] Y. Funakoshi, "Luminosity Tuning at KEKB", in *Proc. eeFACT'16*, Daresbury, UK, Oct. 2016, pp. 147–150. doi:10.18429/JACoW-eeFACT2016-TUT3BH3

[7] D. Zhou, K. Ohmi, Y. Funakoshi, and Y. Ohnishi, "Luminosity performance of superkekb", *Journal of Instrumentation*, vol. 19, no. 02, T02002, Feb. 2024. doi:10.1088/1748-0221/19/02/T02002

[8] P. Kicsiny, X. Buffat, G. Iadarola, T. Pieloni, D. Schulte, and M. Seidel, "Bhabha scattering model for multi-turn tracking simulations at the FCC-ee", in *Proc. IPAC'23*, Venice, Italy, pp. 682–685, Sep. 2023. doi:10.18429/JACoW-IPAC2023-MOPL062

[9] A. Wolski, *Beam dynamics in high energy particle accelerators*. London: Imperial College Press, 2014.

[10] V. Gawas, F. Zimmermann, R. T. Garcia, and X. Buffat, "Modelling Linear Coupling for FCC-ee in Xsuite", in *Proc. IPAC'26, WEP5044, these proceedings*, Deauville, France, May 2026, paper WEP5044, these proceedings.

[11] A. Furman, "Hourglass Effects for Asymmetric Colliders", in *Proc. PAC'91*, San Francisco, CA, USA, May 1991, pp. 422–425.

[12] M. Venturini and W. Kozanecki, "The Hourglass Effect and the Measurement of the Transverse Size of Colliding Beams by Luminosity Scans", in *Proc. PAC'01*, Chicago, IL, USA, Jun. 2001, paper RPPH141, pp. 3573–3575. https://jacow.org/p01/papers/RPPH141.pdf

[13] A. Franchi, E. Métral, and R. Tomás García, "Emittance sharing and exchange driven by linear betatron coupling in circular accelerators", *Phys. Rev. ST Accel. Beams*, vol. 10, p. 064003, 2007. doi:10.1103/PhysRevSTAB.10.064003

[14] DA. Edwards and MJ. Syphers, "An introduction to the physics of high energy accelerators". John Wiley & Sons, Ltd, 1993, pp. 144–171. doi:https://doi.org/10.1002/9783527617272.ch5

[15] K. André, P. Raimondi, S. White, and S. Liuzzo, "Tuning Strategies for the FCC-ee Local Chromaticity Correction Collider Lattice", in *Proc. IPAC'26, MOP1079, these proceedings*, Deauville, France, May 2026, paper MOP1079, these proceedings.